A NUMERICAL STUDY ON EXPLOSIVELY FORMED PROJECTILES IN LOW DENSITY ENVIRONMENTS FOR TYPICAL METALLIC LINERS MATERIALS

Florina BUCUR[1], Liviu-Cristian MATACHE[2]*, Marin LUPOAE[3]

Nowadays, was highlighted an increased need to use special devices for ordnance disposal of various types of unexploded ammunition or improvised explosive device (IED) discovered both in the aquatic and terrestrial environments (on the surface of the soil or buried).

The interventions on these types of ammunition are complicated and complex, any uncontrolled interaction can lead to accidental detonation and disastrous effects on personnel and the surrounding environment. At the world level, various constructive solutions are used to neutralize these threats, in the form of explosive devices generating projectiles, namely explosively formed projectiles (EFPs).

The paper aims to analyze the behavior and influence of liners made of different metallic materials such as copper, aluminum and magnesium in the formation of EFP, highlighting the evolution of the following parameters: shape, formation velocity and kinetic energy in low density environments such as air and water.

Keywords: numerical study, unexploded ordnance, EFP, liner material

1. Introduction

In the context of international armed conflicts, the unexploded ordnance (UXO) or IED that remains in water, soil or underground become deadly threats, conducting to victims among civilians and infrastructure destruction.

The unexploded ammunitions discovered on soil or underwater are generally naval mines, torpedoes, bombs, projectiles, grenades, etc. which did not work according to their intended purpose and which present a high risk of accidental explosion. Also, the improvised explosive devices represent a threat that must be countered [1]. Abandoned ammunitions (AXO) after World War I and World War II and recent international conflicts or ongoing (Afghanistan, Israel, Ukraine), together with unexploded ordnance (UXO) scattered on various environments represent millions of tons of ammunitions (Fig.1). Unexploded ordnance represents a direct threat to communities, infrastructure development, industry, tourism and others.

[1] Assoc. Prof., Military Technical Academy "Ferdinand I", Bucharest, Romania
[2] Prof., Military Technical Academy "Ferdinand I", Bucharest, Romania, *Corresponding author, e-mail: liviu.matache@mta.ro
[3] Assoc. Prof., Military Technical Academy "Ferdinand I", Bucharest, Romania

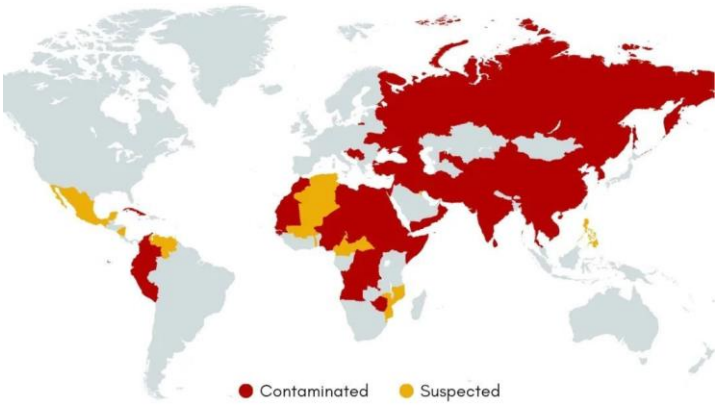

Fig.1. Land mine contaminations map (January 2024) [2]

The neutralization of unexploded ordnance can be accomplished in two ways, by bringing it to the surface and transporting it to a safe area or by applying an explosive ordnance disposal (EOD) procedure at the place where it was discovered, depending on the type of ammunition, the fuse arming, the placement in water or soil etc. [3]. The first way generally applies to ammunition of all types, unarmed, which not present a risk associated with handling and transportation. However, many of the unexploded ordnance are armed and with a high risk of explosion when handled. It is enough to mention the sea mines which, when released into the water, are automatically armed. In addition, some of these have ignition devices that initiate the ammunition when they are in the proximity of some metallic materials. In other words, for these types of ammunition, handling them is out of the question, except for special conditions [4, 5]. These considerations make the second method a safer and more widely used approach.

One of the most used intervention procedures upon an unexploded ammunition involves the penetration of its metal envelope by an explosively formed projectile (EFP), the interruption of the explosive chain and/or the initiation of the ammunition charge deflagration, until it is consumed, or combustion to deflagration of energetic materials occurs. Ammunition that suffers an incomplete detonation, when is subjected to the action of the EFP or when the transition from deflagration to detonation occurs during the initiation of the explosive charge of the non-functioning ammunition, is also considered neutralized [3].

Globally there are a few explosive neutralization devices that must be mentioned: Vulcan Counter-Limpet [6], Pluton [7] and Overload [8].

The neutralization of UXO and IED in specific areas, if transportable, or in the places where they were discovered, is a dangerous operation because of the possible shock waves and fragment propulsion. For this reason, strict rules with a minimum number of operations without moving it from the site where were found, are imposed. The experts have established a clear algorithm for this process that is efficient and safe both for the humans, infrastructures and environment [9].

Because of the sensitive implications of the experimental tests (the risk of projectile initiation during the perforation), to achieve better knowledge regarding the efficiency and the advantages of using EFP, the theoretical approaches are the most appropriate.

If for the case of UXO discovered on soil, there are a series of neutralizing devices, for underwater UXO, environment imposes difficulties, the usual procedures becoming ineffective. For this reason, new methods and devices must be developed.

In the study of phenomena of this type, detonation and blast, a tool often and successfully used is represented by numerical simulations with commercial software available on the market, like Ls-DYNA or Autodyn [10-14].

The design, properties and efficiency of explosively formed penetrators have been subject for different papers [15-19].

The influence of the liner material and explosive type on penetration effectiveness of shaped charge and EFP has been analyzed through numerical and experimental studies [20, 21]. Moreover, several studies are referring to the shape charge section (sub-hemisphere, square, trapezoid etc.) and its influence [22-26].

Also, the behavior of EFP in a denser environment than air, like water, has been studied [27, 28].

Considering a series of experiments, made by the authors, this paper presents a numerical approach regarding the functioning of an EFP neutralizing device type, in low-density environments such as air and water.

To assess the characteristics of the EFP generation and interaction with a projectile shell, a 10 mm thick steel plate representing the body of the non-functional ammunition is used. The impact of projectile configuration with the steel plate and the EFP generation profile were performed through LS-DYNA software. One configuration and three different metallic materials were chosen for the liner: copper, aluminum and magnesium.Based on the data from scientific literature and experimental tests, it has been highlighted that EFPs work best with ductile dense material liners.Copper is chosen because of its wide use, and aluminum and magnesium are two materials with lower shock characteristics.

Also, the potential of metallic materials, like magnesium, to be used in special application due to its properties has been addressed [29-30]. The mechanical properties of chosen metallic liners, allow them to determine specific parameters of EFPs.The numerical study evaluates qualitatively and quantitatively the EFP characteristics by changing the liner materials.

The results from the numerical analysis provide valuable data for the design and development of EFP devices used for UXO neutralization.

2. Problem formulation

2.1 Physical model

Unexploded ordnance or IED neutralization by EFP-generating devices can be applied both for transportable and non-transportable ammunitions.

The main activities are: ammunition identification and risk level evaluation for establishing a safety area, set-up the neutralization device by perforating the metallic body without explosive ignition and burning the explosive with its complete combustion.

When a projectile is located in an unpopulated area, it can also be performed an incomplete detonation, followed by a weak shock wave and propagation of big metallic fragments no more than 5 - 10 m.

The first step of UXO neutralization by EFP implies the generation of a high-velocity projectile that can be accelerated with a velocity up to 4 km/s toward the target, by an explosive detonation.

The general configuration of an EFP device is presented in Fig. 2, where are illustrated steps from projectile generation.

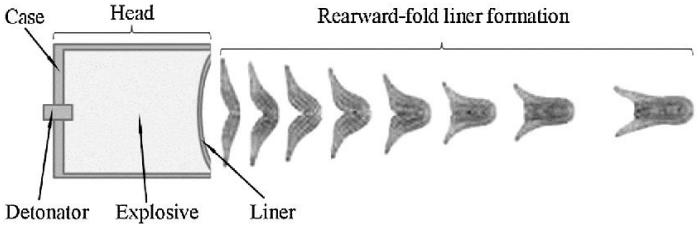

Fig. 2. Configuration and generation of an EFP [9]

The EFP was initially discovered by the oil companies, but in the World War II was used for the perforation of armored vehicles.

Although compared to the cumulative loads it has a smaller perforation distance, the EFP has the advantage of not being dependent of a certain stand-off distance, being able to be used over long distances.

Due to the low velocities and the possibility of using several types of materials as liners, EFPs are successfully used in EOD applications.

In Fig. 3, are presented the main steps for a projectile neutralization using an EFP device.

Fig. 3. Stages of UXO neutralization

Based on authors prior experience, a general physical model of neutralization component is presented in Fig. 4.

The devices analyzed in this paper have cylindrical shape with general dimensions as illustrated bellow. The liner thickness considered is 2 mm.

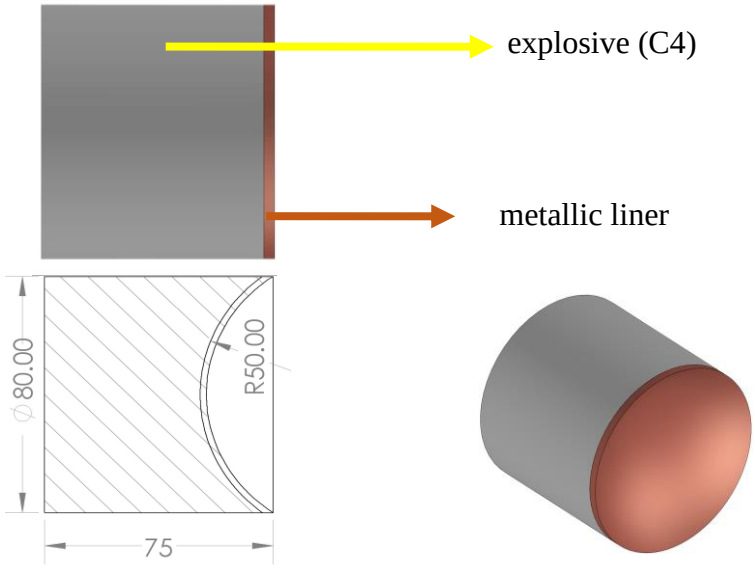

Fig. 4. General neutralization device configuration with dimensions and components

2.2 Virtual model

The numerical simulation of explosively formed projectiles generation was performed through the specialized LS-DYNA software [31].

The geometry of the analyzed model and the testing conditions allow the use of a 2D axis-symmetric simplified model. The virtual model configurations are presented in Fig. 5.

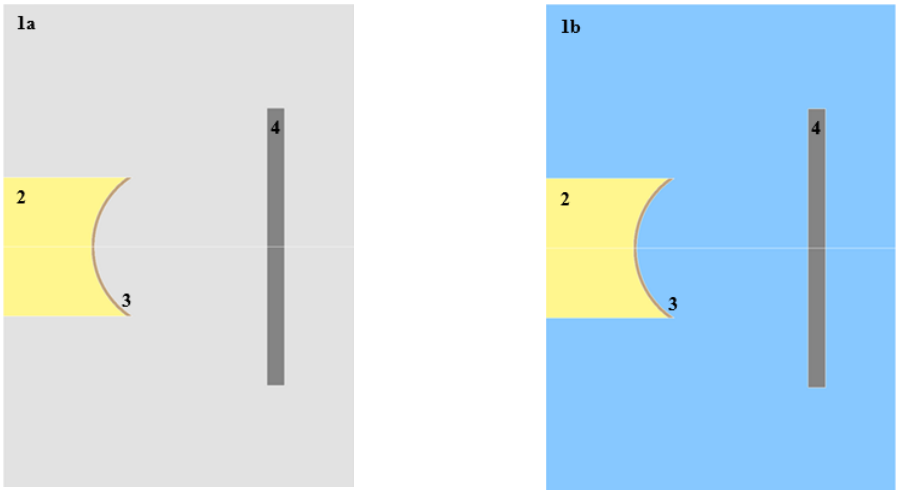

Fig. 5. The virtual model configurations used for neutralization:
1– environment: a – air, b – water, 2 – C4 explosive, 3 – metallic liner, 4 – metallic plate

Explosive used for neutralizing devices is a plastic explosive of C4 type.

For the metallic liner (3), material types are used depending on the ammunition types that need to be neutralized: copper, aluminum and magnesium.

The steel plate has a thickness of 10 mm and is placed at a distance of 75 mm from the base of the explosive charge. The plate thickness was chosen considering an average thickness of the projectile body, and the distance was imposed for reasons of EFP complete generation.

The analysis was performed for devices that were disposed in two different environment, air and water.

The virtual models were created using axial symmetric plane quadrilateral elements of SHELL 15 type with weighting of the functions by volume. A number of 46480 elements and 47111 nodes were obtained.

The liner (3) and the metallic plate (4) were modeled using Lagrange elements, and for the explosive and low-density environments through which the EFP propagates, Euler elements were used.

The interaction between the components was realized with the *CONSTRAINT_LAGRANGE_IN_SOLID command.

The metallic plate was constrained on the exterior contours.

The material models introduced in the program for Lagrange simulated structures are: for copper, aluminum, magnesium liners and steel plate a material model of type *MAT_PLASTIC_KINEMATIC, and for Euler simulated environment (air and water) a *MAT_NULL type material model was used.

Erosion failure criteria used for steel plate was effective plastic strain.

The material models used along with the specific parameters for each material are detailed in the Table 1.

Table 1

Material parameters [29]

Material	Density [g/cm^3]	Young Modulus MPa]	Poisson ratio	Yield strength [MPa]	Tangent modulus [MPa]	Effective plastic strain
Copper	8.96	1.2e+5	0.33	100	100	-
Aluminum	2.7	6.8e+4	0.32	95	90	-
Magnesium	1.81	4.52e+4	0.35	20	70	-
Steel	7.75	2.1e+5	0.27	1850	3626	1.1

Material	Density [g/cm^3]	Pressure cutoff [MPa]
Air	1.23e-3	1e-6
Water	0.998	

For the explosive material and studied environments, equations of state like Jones-Wilkins-Lee, Mie–Grüneisen and polynomial type, were also used.

For high explosives detonation products, the JWL equation of state used is [32]:

$$P = A\left(1-\frac{\omega}{R_1 V}\right)e^{-R_1 V} + B\left(1-\frac{\omega}{R_2 V}\right)e^{-R_2 V} + \frac{\omega E}{V} \tag{1}$$

where A, B, C, R_1, R_2, and ω are material constants, $V = \frac{v}{v_0}$ is the product volume relative to the initial explosive volume, E is the energy per unit volume, and p is the pressure.

For water, the behavior is described by Mie–Grüneisen equation of state [32]. The pressure is defined for compressed materials by a cubic shock-velocity as a function of particle velocity $v_s\left(v_p\right)$:

$$p=\frac{\rho_0 C^2\mu\left[1+\left(1-\frac{\gamma_0}{2}\right)\mu-\frac{a}{2}\mu^2\right]}{\left[1-\left(S_1-1\right)\mu-S_2\frac{\mu^2}{\mu+1}-S_3\frac{\mu^3}{\left(\mu+1\right)^2}\right]}+\left(\gamma_0+a\mu\right) \tag{2}$$

and for expanded materials as:

$$p=\rho_0 C^2\mu+\left(\gamma_0+a\mu\right)E \tag{3}$$

where C is the intercept of the $v_s\left(v_p\right)$ curve, S_1, S_2, and S_3 are the unitless coefficients of the slope of the $v_s\left(v_p\right)$curve, γ_0 is the unitless Gruneisen gamma, a is the unitless, first order volume correction to γ_0, and $\mu=\frac{\rho}{\rho_0}=1$.

The air behavior is defined by the linear polynomial equation of state, linear in internal energy, pressure being [25]:

$$p=C_0+C_1\mu+C_2\mu^2+C_3\mu^3+\left(C_4+C_5\mu+C_6\mu^2\right) \tag{4}$$

The terms $C_2\mu^2$ and $C_6\mu^2$ are 0 if $\mu<0$, $\mu=\frac{\rho}{\rho_0}=1$, where $\frac{\rho}{\rho_0}$ is the ratio of current density to reference density. The reference (nominal) density is introduced in the *MAT_NULL card.

Equation (4) may be used with the gamma law equation of state to model the gas, by imposing $C_0=C_1=C_2=C_3=C_6=0$ and $C_4=C_5=\gamma-1$. The ratio specific heat is $\gamma=\frac{C_p}{C_v}$.

Pressure for a perfect gas is defined by $p=\left(\gamma-1\right)\frac{\rho}{\rho_0}E$ (E has unit of pressure).

The constants involved in the equations of state above are those specific of the C4 explosive, air and water as presented in the specialty literature (Table 2).

Table2

Material constants [32]

Material	A	B	R1	R2	OMEGA	E0	V0
C4	7.783e+5	7071	4.2	1	0,3	1.05e+4	1

Material	C0	C1	C2	C3	C4	C5	C6	E0	V0
Air					0.4	0.4	0	0.2895	1

Material	C	S1	S2	S3	Gama0	A	E0	V0
Water	1.647e+4	1.921	-0.096	0	0.4	0.4	0.2895	1

The detonation of the explosive was carried out similarly like a blasting cap functioning, which was centrally inserted into the explosive.

Contact option, *CONTACT_2D_AUTOMATIC_SURFACE_TO SURFACE, was imposed between the Lagrange modeled materials (EPF and steel plate).

3. Results and discussions

The numerical study was able to predict for the explosively formed projectile, the shape, the velocity and the kinetic energy.

An important parameter that influences the process is the explosive pressure after the detonation. The iso-values for pressure field are presented in Fig. 6.

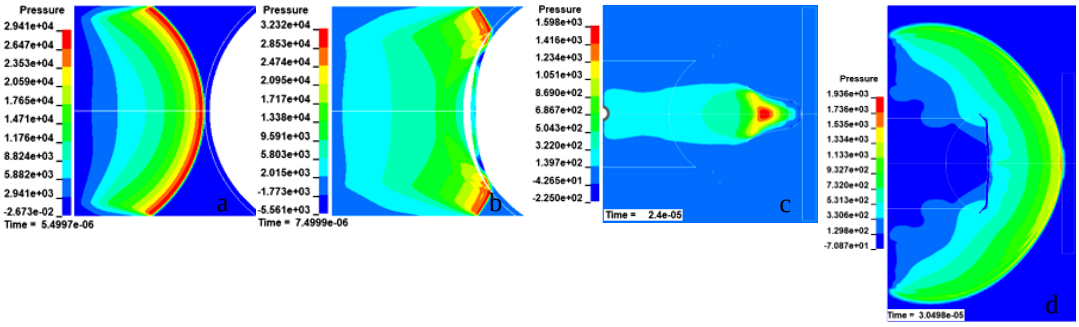

Fig. 6. Pressure evolution [MPa] after C4 explosive initiation (a, b – detonation wave in explosive, c – shock wave in air, d – shock wave in water)

First parameter observed for the neutralization device proposed is the EFP generation evolution, respectively the projectile shape for each studied liner and environment: copper liner in air and water (Fig. 7, Fig. 8), aluminum liner in air and water (Fig. 9, Fig.10) and magnesium liner in air and water (Fig. 11, Fig.12).

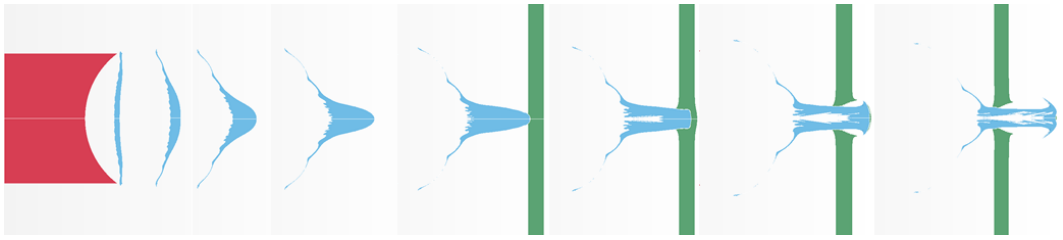

Fig. 7. EFP generation in air for copper liner at successive time moments (s): 1.4e-05, 1.95e-05, 2.6e-05, 3.15e-05, 3.6e-05, 3.9e-05, 4.5e-05, 5.35e-05

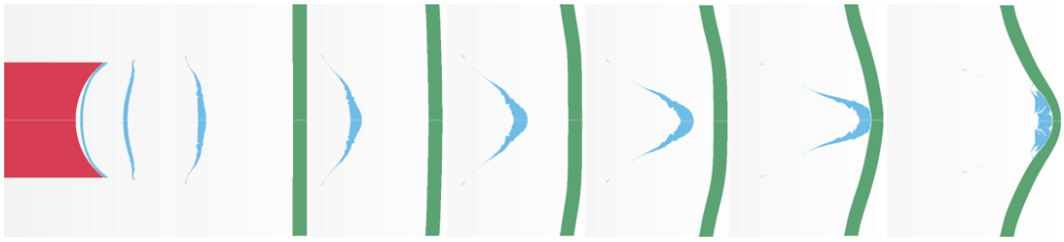

Fig. 8. EFP generation in water for copper liner at successive time moments (s): 8e-06, 1.85e-05, 3.5e-05, 4.85e-05, 6.95e-05, 9e-05, 0.00012, 0.00022

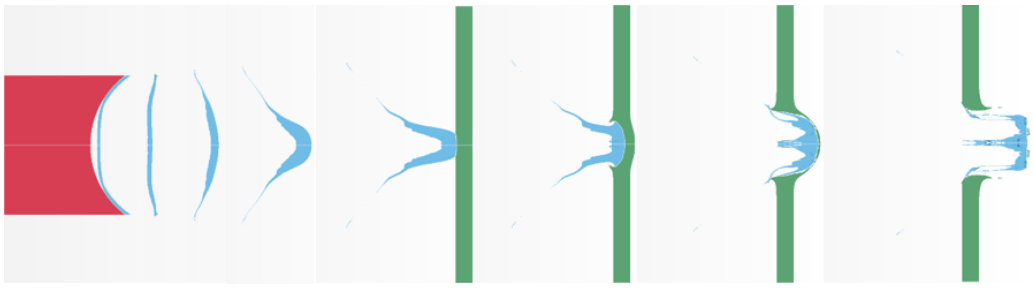

Fig. 9. EFP generation in air for aluminum liner at successive time moments (s): 7e-06, 1.05e-05, 1.45e-05, 2.05e-05, 2.65e-05, 2.95e-05, 3.65e-05, 4.3e-05

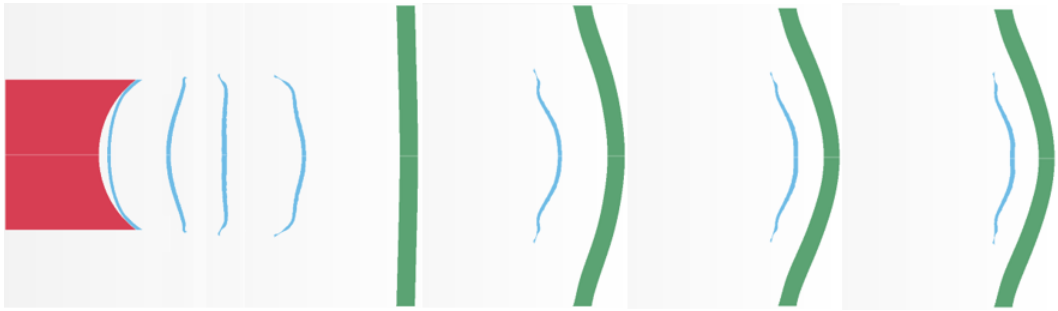

Fig. 10. EFP generation in water for aluminum liner at successive time moments (s): 8e-06, 1.5e-05, 2.55e-05, 4.35e-05, 0.00012, 0.00019, 0.0003

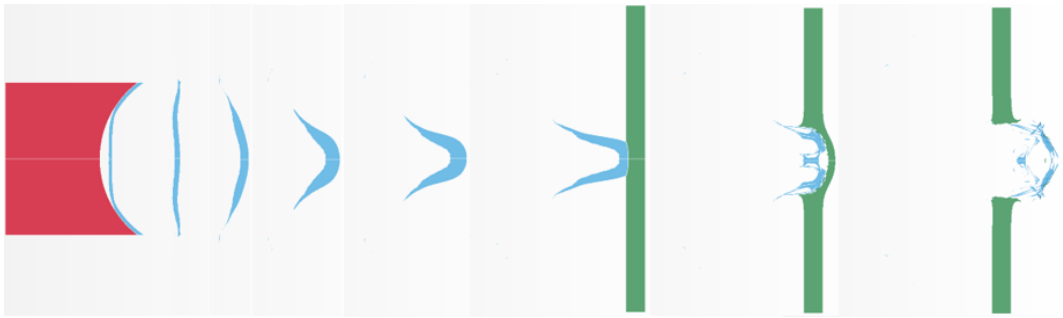

Fig. 11. EFP generation in air for magnesium liner at successive time moments (s): 7e-06, 1.05e-05, 1.4e-05, 1.85e-05, 2.15e-05, 2.5e-5, 3.05e-05, 4.05e-05

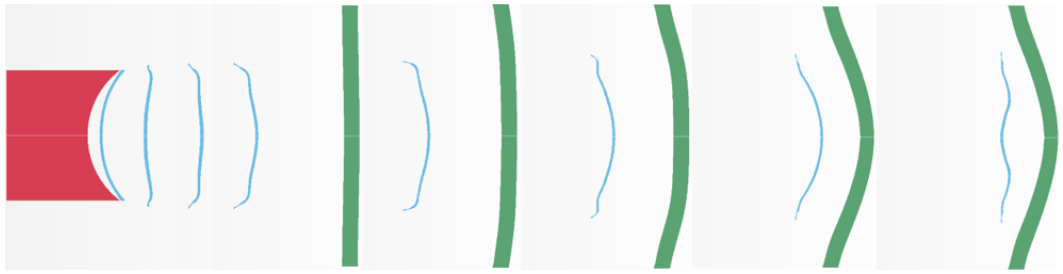

Fig. 12. EFP generation in water for magnesium liner at successive time moments (s): 9.5e-06, 2.15e-05, 3.05e-05, 3.95e-05, 6.1e-05, 9.1e-05, 0.00015, 0.00026

For air studied cases, the formation of EFP and the perforation of the steel plate can be observed for all types of liners (Fig. 7, Fig. 9, Fig. 11).

In the water studied cases, the EFP is formed only for copper liner, the other two types (aluminum and magnesium) no longer lead to the formation of EFP (Fig. 8, Fig. 10, Fig. 12).

Regarding the parameters that describe the process determined by liner type, EFP velocity (Fig. 13-15) and EFP kinetic energy evolution (Fig. 16-18) were plotted for the two environments studied.

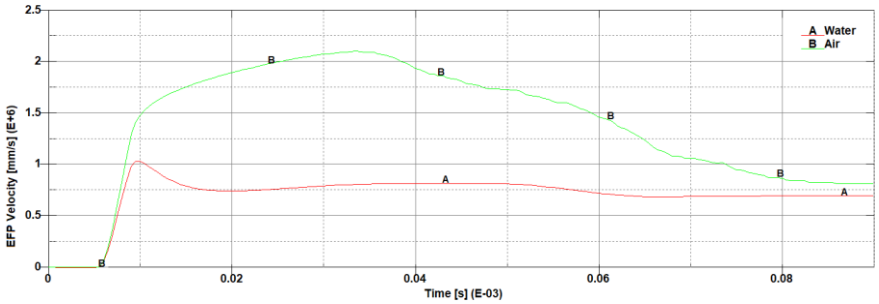

Fig. 13. EFP velocity evolution for copper liner

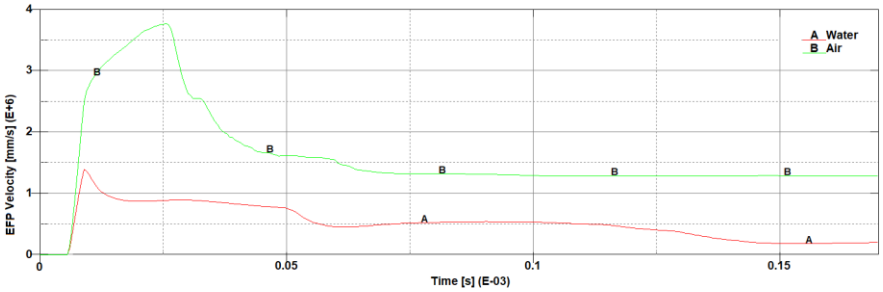

Fig. 14. EFP velocity evolution for aluminum liner

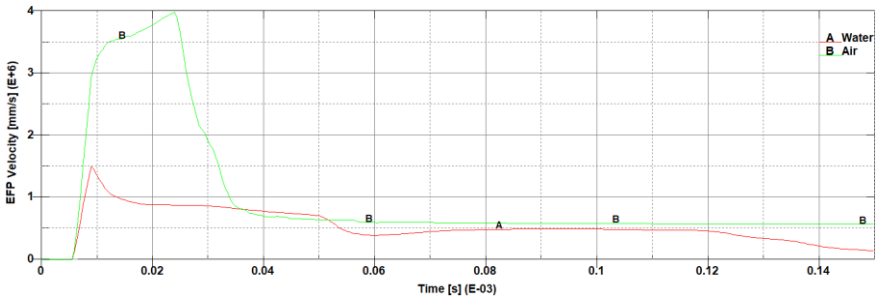

Fig. 15. EFP velocity evolution for magnesium liner

It can be observed, that in air, the EFP velocities have values higher than the ones in water, with maximum values between 2 km/s and 4 km/s (higher for aluminum and magnesium), while for the kinetic energy the maximum values are between 35 - 45 kJ, higher for copper and aluminum.

In water, the maximum EFP velocities have values between 1 km/s and 1.5 km/s, and the values for EFP kinetic energy are between 5 - 14 kJ.

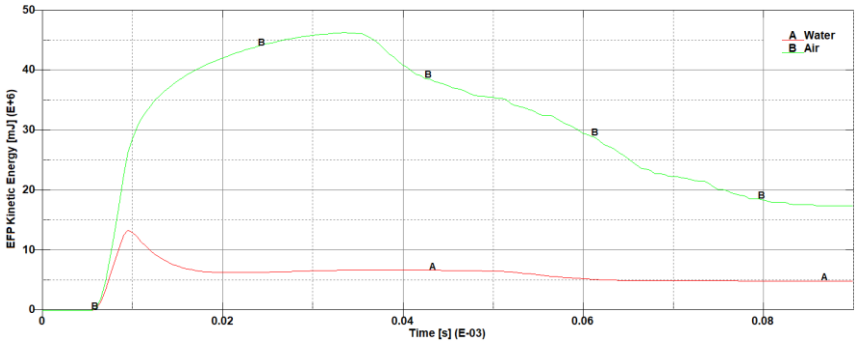

Fig. 16. EFP kinetic energy evolution for copper liner

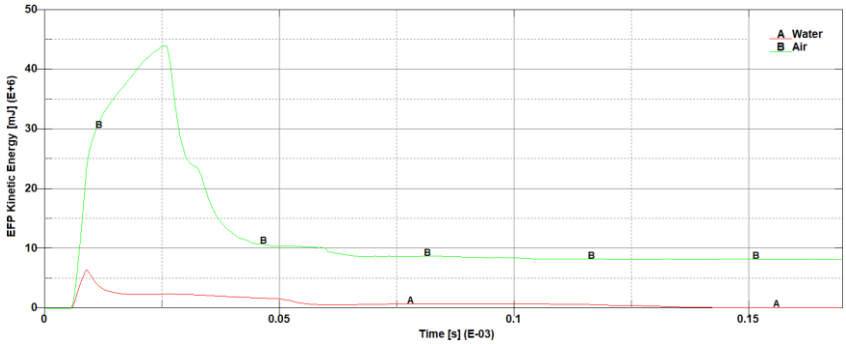

Fig. 17. EFP kinetic energy for aluminum liner

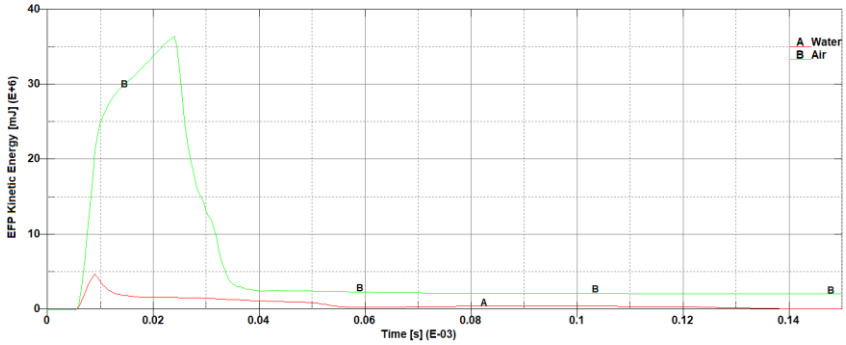

Fig. 18. EFP kinetic energy evolution for magnesium liner

The steel plate behavior was analyzed in terms of kinetic energy evolution in the two studied environments (Fig. 19-21).

It can be noticed that, in water, the plate kinetic energy for copper liner is higher than in the air, even if the plate is not perforated. This is explained by the fact that in water, the EFP is generated and hits the plate. For the other liners, aluminum and magnesium, the plate kinetic energy is higher in the air, because the EFPs are no longer formed and also do not interact with the steel plate, being also decelerated by the water.

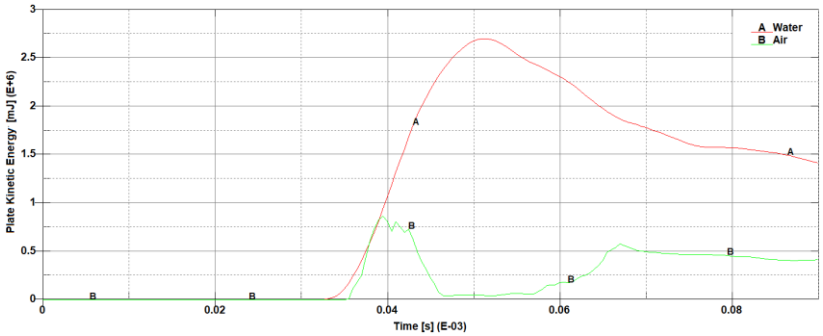

Fig. 19. Metallic plate kinetic energy evolution in case of copper liner

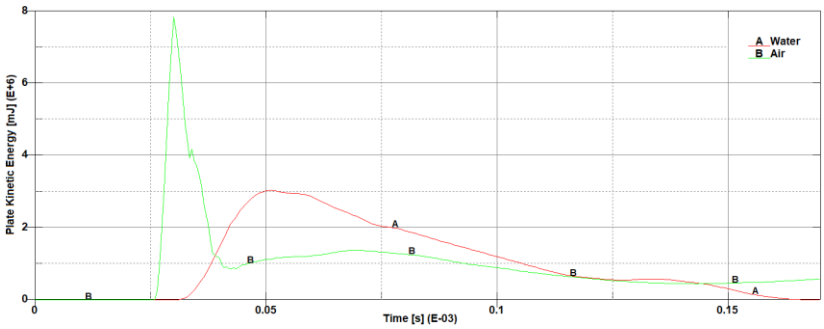

Fig. 20. Metallic plate kinetic energy evolution in case of aluminum liner

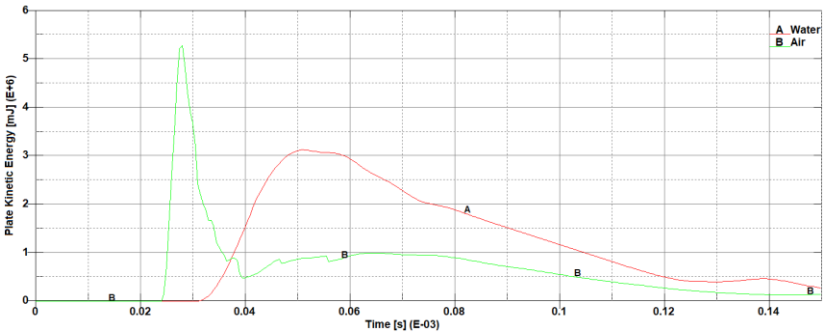

Fig. 21. Metallic plate kinetic energy evolution in case of magnesium liner

4. Conclusions

Considering the international context, military applications of neutralizing non-functioning military ammunitions that can be located (intentionally or non-intentionally) on the soil or underwater has become a subject of intense study.

This numerical study which derived from military applications of unexploded ordnance neutralization focuses on observing the behavior and mechanism of EFP formation for three different metallic liner materials (copper, aluminum and magnesium), in two different density environments (air and water). The hemispheric liners were tested on a steel plate.

The results were obtained through Ls-DYNA software. The numerical models used were able to predict the EFP formation and the plate perforation.

The analyzed parameters were shape, velocity and kinetic energy for the EFP, and also the kinetic energy for the metallic plate.

Qualitatively it can be observed that in the water, the EFP form differs more and more as the density and mechanical properties of the liner decrease, the copper having approximately the same shape as the one in the air, while the aluminum and magnesium does not form, environment being much denser than air.

At the same time, it can be observed that the high propagation velocity of the shock wave in the water causes the wave produced by the explosive detonation to arrive before the EFP to the plate, causing its bending.

This fact leads to the difficulty of perforating the plate, the EFP hitting the curved plate in the case of the copper liner.

For the aluminum and magnesium liner, it's noticeable that not only is the EFP no longer formed, but the liner also undergoes deceleration before impacting the steel plate.

Also, the EFP velocity and kinetic energy have much lower values in water, than in air.

In this regard, for the efficiency of the neutralization systems in the aquatic environment, it is necessary to isolate the space between the liner and target in order to allow the EFP to reach the optimal shape and velocity.

Furthermore, for water case, it can be mentioned that if the density of the material used for the liner increases, the plate perforation may occur.

Also, in the context of its efficiency, the potential of using explosively formed projectile for civilian applications must also be studied.

R E F E R E N C E S

[1]. https://www.icrc.org/en/document/five-things-to-know-about-deadly-legacy-explosive-remnants-war

[2]. https://mapsontheweb.zoom-maps.com/post/739419757981335552/landmine-contamination-by-worldinmaps

[3]. Unexploded Ordnance (Uxo) Procedures, Field Manual No. 4-30.51 (21-16), MCRP 3-17.2A, Department of the Army Washington, DC, 13 July 2006

[4]. https://www.gichd.org/fileadmin/GICHD-resources/rec-documents/Guide-Underwater-Clearance-June2016.pdf

[5]. https://www.escgs.com/services/underwater-works/uxo-clearance..

[6]. https://www.explosives.net/vulcan-counter-limpet-mine-system

[7] https://static1.squarespace.com/static/5f5782157a79a6713d7c551b/t/6017e7578d4d172b1501d096/1612179317555/PL-D200-05-Pluton-Datasheet.pdf

[8]. https://www.suprameca.com/en/supralod

[9]. https://en.wikipedia.org/wiki/Unexploded_ordnance

[10]. *L. Matache, C. Puică, A. Rotariu, E. Trană, F. Bucur,* "Numerical simulation of military ground vehicle's response to mine-blast load", UPB Scientific Bulletin, Series D: Mechanical Engineering, **vol. 80**, no 4, 2018, pp. 153-162.

[11]. *E. Trană, F. Bucur, A. Rotariu*, "On the fragmentation of explosively-driven plastic/steel layered cylinders", Materiale Plastice, **vol. 55**, no.4, 2018, pp. 521-523.

[12]. *Chiriac, O. Bucur, F. Rotariu, A.-N. Trană, E.* "The Application of Mott's Distribution in the Fragmentation of Steel Coaxial Cylinders", Materials, **vol 16**, 5783, 2023.

[13]. *C. Enache, E. Trană, T. Rotariu, A. Rotariu, V.- T. Țigănescu, T. Zecheru*, "Numerical simulation and experimental tests on explosively-induced water jets phenomena", Propellants, Explosives, Pyrotechnics, **vol. 41**, no 6, 2016, pp. 1020-1028.
[14]. *M. Lupoae, C. Baciu, D. Constantin*, "Metallic doors under explosive charges detonation, ICMT 2017 - 6th International Conference on Military Technologies", 7988769, 2017, pp. 273–277.
[15]. *C.A. Weickert, P.J. Gallagher*, "Penetration of explosively formed projectiles", International Journal of Impact Engineering, **vol. 14**, no. 1–4, 1993, pp. 809-818.
[16]. *S. Miller*, "A new design criteria for explosively-formed hypervelocity projectile (EFHP)", Int. J. Impact Eng., 10(1e4):403e11, 1990.
[17]. *J. Houman, Z. Ruoqi, Z. Shouqi*, "Application of nonlinear programming to explosively formed projectile design", J. Phys. IV, 10(PR9). Pr9-451-Pr9- 456, 2010.
[18]. *S. Pappu, L.E. Murr*, "Hydrocode and microstructural analysis of explosively formed penetrators, J Mater Sci, **vol. 37, no.** 2:233e48, 2002, pp. 233–248.
[19]. J. *Wu, J. Liu, Y. Du*, "Experimental and numerical study on the flight and penetration properties of explosively-formed projectile", Int. J. Impact Eng., **vol. 34**, no 7:1147e62, 2007.
[20]. *S. Zaki, E. Uddin, B. Rashid, A. Mubashar, S.R. Shah*, "Effect of liner material and explosive type on penetration effectiveness of shaped charge", Proceedings of the Institution of Mechanical Engineers, Part L: Journal of Materials: Design and Applications, **vol. 233**, no. 7, 2019, pp. 1375-1383.
[21]. *J.F. Liu, Y. Long, C. Ji, M. Zhong, Q. Liu*, "The influence of liner material on the dynamic response of the finite steel target subjected to high velocity impact by explosively formed projectile", Int. J. Impact Eng., 109:264–75, 2017.
[22]. *Tian-bao Ma, Jing Liu, Qi Wang*, "Influence of shaped charge structure parameters on the formation of linear explosively formed projectiles", Defence Technology, **vol. 18**, 1863e1874, 2022.
[23]. *P. Zochowski, R. Warchoł,* "Experimental and numerical study on the influence of shaped charge liner cavity filing on jet penetration characteristics in steel targets", Def. Technol. 2022.
[24]. *Z. H. Yao, D. Z. Li, Q. H. Fu, C. Wu*, "Numerical Simulation of Shaped Charge with an Eccentric Sub-hemisphere Liner", Explosive Materials, **vol. 42**, no. 2, 2013, pp. 17-20.
[25]. *Y. Wang, Z. Huang, X. Zu, B. Ma, Y.E. Cai*, "Experimental Study on Jet Formation and Penetration Characteristics of Square cross-section Shaped Charge", Lat. Am. J. Solids Struct., **vol. 18**, 2021.
[26]. *M. Bin, Z. Huang, Y. Wu, Y. Wang, X. Jia, G. Gao*, "Research on the Formation Characteristics of the Shaped Charge Jet from the Shaped Charge with a Trapezoid Cross-Section", Materials, **vol. 15**, no. 23: 8663, 2022.
[27]. *C. Huang, M. B. Liu, B. Wang, Y. P. Zhang*, "Underwater explosion of slender explosives: Directional effects of shock waves and structure responses", Int J. Impact. Eng., 130:266–80, 2019.
[28]. *C. Lam, D. McQueen*, Study of the Penetration of Water by an Explosively Formed Projectile, DSTO Aeronautical and Maritime Research Laboratory, Melbourne Victoria 3001 Australia, 1998.
[29] *I. Antoniac, M. Miculescu, V. Manescu, A. Stere, PH Quan, G. Paltanea, G, A. Robu, K. Earar*, "Magnesium-Based Alloys Used in Orthopedic Surgery", Materials, **vol. 15**, no 13, 1148, 2022.
[30] *I. Antoniac, V. Manescu (Paltanea), A. Antoniac, G. Paltanea*, "Magnesium-based alloys with adapted interfaces for bone implants and tissue engineering", Regenerative Biomaterials, **vol. 10**, 2023.
[31]. ***LS-DYNA® Keyword users's manual 971
[32]. *B.M Dobratz*, LLNL Explosives Handbook, Properties of Chemical Explosives and Explosive Simulants, US Department of Commerce, National Techn. Information Service, 1981.